

Geometrical optimization of pumping power under adiabatic parameter driving

Masahiro Hasegawa and Takeo Kato

Institute for Solid State Physics, The University of Tokyo, Kashiwa, Chiba 277-8581, Japan

(Dated: December 15, 2024)

Adiabatic pumping is one of the fundamental concepts in time-dependent transport of mesoscopic devices. To maximize the performance of pumping, i.e., the amount of pumping per unit time, we need special care on the speed of the driving, because it should be sufficiently slower than a *limited speed*, an upper bound of the driving speed below which non-adiabatic effects are negligible. In general, the amount of pumping increases as the contour of the driving parameter becomes longer, while a long contour is disadvantageous to the pumping power as it takes much time per cycle under the constraint of the *limited speed*. We consider this trade-off relation carefully, and show that there should exist an optimized period and contour to maximize the power of adiabatic pumping. We demonstrate our conclusion in charge pumping via a single-level quantum dot.

I. INTRODUCTION

Adiabatic pumping, which is one of transport phenomena induced by quasi-static periodic parameter driving, has been attracting great interest since the first proposal by Thouless¹. In the field of mesoscopic physics, electron turnstile and pumping were studied both theoretically and experimentally by a number of researchers²⁻⁶. For electronic transport via non-interacting quantum systems, the charge transferred by adiabatic pumping is written in terms of the Berry curvature defined from the scattering matrices, which is known as Brouwer's formula⁷. This geometrical framework has been generalized to adiabatic charge pumping in various electron systems⁸⁻¹⁵. It is also worth noting that recent development in experimental techniques has been encouraging us to study adiabatic heat pumping via nanoscale devices¹⁶⁻¹⁹.

Adiabatic pumping has also been studied as a basic concept of quasi-static operations in non-equilibrium steady state thermodynamics²⁰. Steady state entropy production induced by quasi-static operations was formulated for general systems in a geometrical manner^{21,22}, and an entropy of non-equilibrium steady states was proposed for quantum dot systems²³ and harmonic oscillator systems²⁴. The performance of quantum engines utilizing nanoscale devices has also been studied in phonon systems²⁵ and double quantum dot systems¹⁷. The discussion of the performance of quantum engines has been recently developed to the non-adiabatic and non-equilibrium region. The trade-off relation between power and efficiency of engines has been gathering attention^{26,27}.

Adiabatic pumping can be utilized for various applications such as electron pump, heat pump, refrigerator, and so on. One important indicator on performance of such pumping devices is a power, i.e., a transfer rate of pumped quantities (heat or charge) per unit time. In order to increase the power of adiabatic pumping, there are three factors: (a) speed of driving, (b) shape of a pumping contour in parameter space, and (c) leakage current.

Let us discuss each factor one by one as follows.

It is known that the amount of charge or heat transferred in one adiabatic cycle is constant and independent of the speed of driving, as long as the contour of pumping in the parameter space is fixed. Therefore, the power of the adiabatic pumping is proportional to the driving frequency. There is, however, an upper limit of the speed determined by the condition of the adiabatic approximation; the parameters should be driven quasi-statically. If the parameters are driven quickly, non-adiabatic corrections become significant and the geometrical description of adiabatic pumping collapses. Therefore, the pumping power of adiabatic pumping should be maximized under the constraint that the speed of driving must be below the *limited speed*, i.e., the upper bound below which non-adiabatic corrections is negligible (for precise discussion, see Appendix A).

The second factor, the shape of the contour loop in the parameter space, directly determines the pumping power via Brouwer's formula⁷, in which the amount of charge or heat transferred in one cycle is expressed by a surface integral of the Berry curvature for an area enclosed by the contour. We note that the pumping power is written in terms of the Berry curvature even for interacting electron systems^{10,14,15} (see Appendix A). The amount of pumping per one cycle increases when the contour encloses a wide area on which the Berry curvature takes a large value. It seems that the maximum power of pumping is realized if the area enclosed by the trajectory is widened as possible. However, this strategy fails because the speed of driving must be below the *limited speed* mentioned in the previous paragraph. Although the amount of pumping in one cycle increases for a large contour, the period of one cycle is proportional to the length of the contour under the condition that the driving speed is set as a constant value below the *limited speed*. Therefore, the pumping power may become small when the contour length is too large. This indicates that there exists an optimal contour and period to maximize the pumping power (see Fig. 1). This is the main subject of this paper.

The third factor, the leakage current, also affects the optimal contour. Charge(heat) pumping devices may

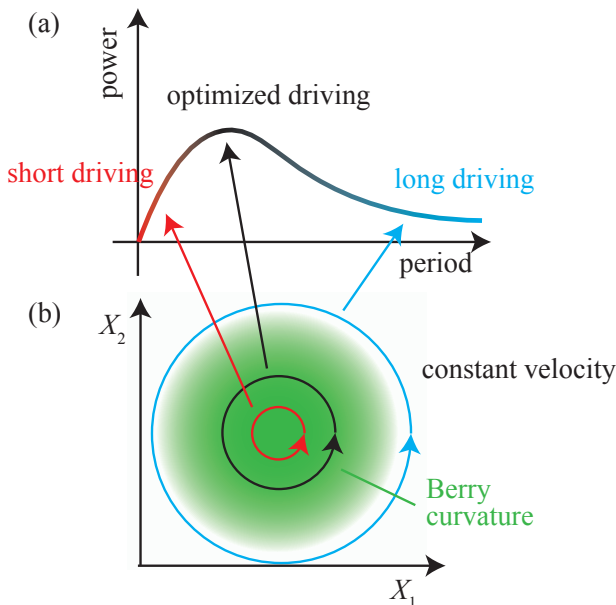


FIG. 1. (a) A schematic graph of the pumping power as a function of the period of one cycle. (b) Examples of the contours in the parameter space, where X_1 and X_2 denote the driving parameters, and the density map plot (green) shows the Berry curvature as a function of (X_1, X_2) . For short contours, the adiabatic pumping per cycle, which is characterized by an integral of the Berry curvature on the area enclosed by the contour, is so small that the pumping power is suppressed. The pumping power is also reduced for long contours, because the pumping period becomes large. Therefore, there exists the best driving period with the optimized contour to maximize the power.

be operated against a finite bias for chemical potentials or temperatures. In such a biased system, the leakage charge(heat) current flows in the direction opposite to that of pumping. The leakage current is given by the time integral on the contour, and depends on both the cycle period and the amplitude of the leakage current. Therefore, to suppress the leakage current under a fixed speed of driving as possible, the optimal contour should be modified to shorten its length or avoid the parameter region on which leakage current is large.

Our purpose of this paper is summarized as follows. We consider optimization of the power in adiabatic pumping under the constraint that the driving speed is below the *limited speed*, which guarantees adiabaticity in system dynamics induced by the parameter driving. By taking a long contour, the amount of pumping per one cycle can be increased, while the pumping rate (the number of cycles per unit time) should be reduced. The large contour is also disadvantageous for the pumping power because of increase of the leakage current flowing against the pumping direction. Taking these factors into account, we consider the optimization problem for general types of pumping. We also demonstrate the existence of the

optimal contours by a simple example of electron pumping through a non-interacting single-level quantum dot. Our discussion is restricted to the trade-off relation between the amount of adiabatic pumping and the pumping period, which should be distinguished from the trade-off relation discussed in Ref. 27.

This paper is organized as follows: In Sec. II, we introduce a general framework for optimizing the pumping power. In Sec. III, we discuss the adiabatic charge pumping via a single-level quantum dot system using approximate calculation. In Sec. IV, we summarize our results.

II. FORMALISM

In this section, we introduce a general framework for optimizing the pumping power. For simplicity, we consider two-parameter pumping although it is straightforward to extend the present framework into pumping by more than two parameters. Throughout this paper, we employ the unit of $\hbar = 1$.

A. Adiabatic approximation

We consider pumping induced by two-parameter driving described by the dimensionless parameter vector, $\mathbf{X}(t) = (X_1(t), X_2(t))$. The parameter driving is periodic in time, i.e., $\mathbf{X}(t + \mathcal{T}) = \mathbf{X}(t)$, where \mathcal{T} is a period of the pumping cycle. We employ the adiabatic approximation^{7,10,14,15} assuming that the parameter driving is sufficiently slow in comparison with characteristic time scales of the system. In this approximation, the amount of charge or heat transferred in one cycle, Q , is given by a sum of two contributions:

$$Q \simeq Q^{\text{st.}} + Q^{\text{ad.}}, \quad (1)$$

$$Q^{\text{st.}} = \int_0^{\mathcal{T}} dt j[\mathbf{X}(t)], \quad (2)$$

$$Q^{\text{ad.}} = \int_A dX_1 dX_2 \Pi(\mathbf{X}), \quad (3)$$

where $Q^{\text{st.}}$ is a total amount of a steady-state leakage current in one cycle, $Q^{\text{ad.}}$ is a contribution of adiabatic pumping, $j[\mathbf{X}(t)]$ is the steady-state leakage current, and $\Pi(\mathbf{X})$ is the Berry curvature. Eq. (3) is known as Brouwer's formula⁷, in which the transferred heat or charge is written by the surface integral of $\Pi(\mathbf{X})$ for the two-dimensional area A enclosed by the driving contour $C = \{\mathbf{X}(t) | 0 \leq t < \mathcal{T}\}$ (for detail derivation, see Appendix A). The steady-state leakage depends on the driving speed of $\mathbf{X}(t)$, whereas the contribution of adiabatic pumping is independent of it.

B. Optimization functional

We introduce a dimensionless parameter s to parametrize the contour, $C = \{\mathbf{X}(s) | 0 \leq s < 1\}$, and rewrite the time integral as

$$\int_{t_i}^{t_f} dt \rightarrow \int_0^1 ds \tau(s), \quad (4)$$

where $\tau(s) = dt/ds$ is a function of s . We note that $\tau(s)ds$ denotes a dwell time on the contour interval $[s, s + ds]$, and depends on the speed of the parameter driving. For simplicity, as described in the introduction, we assume that the driving velocity $v = |d\mathbf{X}/dt|$ is constant. Then, the amount of transferred charge or heat in one cycle, Q , is given by a functional of the contour C as

$$Q[C] = \int_0^1 ds l(s)U[\mathbf{X}(s)] + \int_A dX_1 dX_2 \Pi(\mathbf{X}). \quad (5)$$

where $l(s) = v\tau(s)$, and $U[\mathbf{X}(s)]$ is the normalized leakage current defined as

$$U[\mathbf{X}(s)] = v^{-1}j[\mathbf{X}(s)]. \quad (6)$$

For optimization of adiabatic pumping under the fixed driving period \mathcal{T} , we introduce a functional with the Lagrange multiplier as

$$Z[C, \mathcal{T}] = Q[C] + \lambda \left[v^{-1} \int_0^1 ds l(s) - \mathcal{T} \right], \quad (7)$$

where λ is the Lagrange multiplier. Using the optimized contour C_{opt} which maximizes $Z[C, \mathcal{T}]$, the total pumping power P is defined as

$$P(\mathcal{T}) = \frac{Z[C_{\text{opt}}, \mathcal{T}]}{\mathcal{T}}. \quad (8)$$

Our main purpose is to clarify whether the ‘best’ period \mathcal{T}_{max} to maximize the performance of pumping, i.e., $P(\mathcal{T})$ exists or not.

III. SINGLE-LEVEL QUANTUM DOT SYSTEM

In this section, we consider the performance of pumping in a specific setup, i.e., electron pumping via a single-level quantum dot (see Fig. 2), and show that there indeed exists an optimizing period which maximizes the pumping power. Since the optimal period is obtained by a simple mechanism (see also Sec. I), we can sufficiently expect that the present result holds also for general systems.

A. Model

The Hamiltonian, which describes charge transport via a single-level quantum dot, is given as

$$H(t) = H_d(t) + H_t(t) + \sum_{r=L,R} H_r, \quad (9)$$

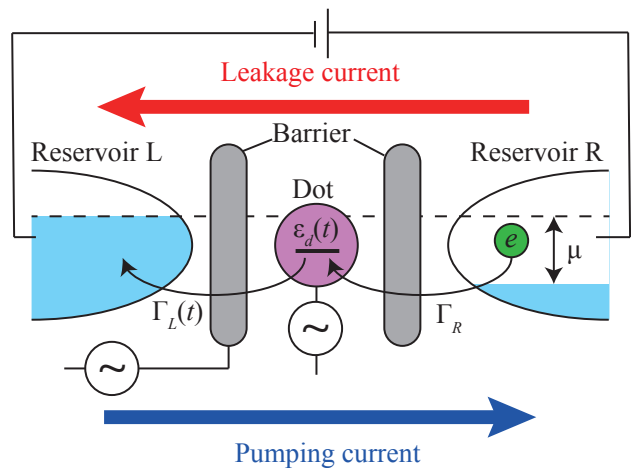


FIG. 2. A schematic of the single-level quantum dot system. A quantum dot and two electron reservoirs, reservoir L and R , are separated by potential barriers and coupled to each other by electron tunneling. The energy level in the quantum dot, $\epsilon_d(t)$, and the coupling between the dot and the reservoir L , $\Gamma_L(t)$, is taken as time-dependent driving parameters. The bias between reservoirs is expressed by a chemical potential difference μ . The leakage current induced by the bias flows from the reservoir R to the reservoir L , while the charge is pumped in the opposite direction (note that the direction of the electron transfer is opposite). The sign of the current is defined as positive for the pumping current (the blue arrow) and negative for the leakage (the red arrow).

where

$$H_d(t) = \epsilon_d(t)d^\dagger d, \quad (10)$$

$$H_t(t) = \sum_k [v_L(t)c_{Lk}^\dagger d + v_R c_{Rk}^\dagger d + h.c.], \quad (11)$$

$$H_r = \sum_k \epsilon_k c_{rk}^\dagger c_{rk}. \quad (12)$$

Here d (d^\dagger) denotes the annihilation (creation) operator of an electron in the quantum dot, c_{rk} (c_{rk}^\dagger) denotes the annihilation (creation) operator of electrons in the reservoir $r = L, R$ with wave number k and energy ϵ_k . In our model, we assume that the energy level of the quantum dot, $\epsilon_d(t)$, and one of the dot-reservoir couplings, $v_L(t)$, are time-dependent driving parameters, whereas the other dot-reservoir coupling, v_R , is taken as constant. We further assume that both of the reservoirs are kept at zero temperature, and their Fermi distribution functions are given as

$$f_L(\epsilon) = \Theta(\epsilon - \mu/2), \quad f_R(\epsilon) = \Theta(\epsilon + \mu/2), \quad (13)$$

where $\Theta(\epsilon)$ is the Heaviside step function, and the average of the Fermi energies of the two reservoirs is set to zero. In the wide-band limit, the linewidth of the energy

level in the quantum dot is given as $\Gamma_L(t) + \Gamma_R$, where

$$\Gamma_L(t) = \pi\rho|v_L(t)|^2, \quad (14)$$

$$\Gamma_R = \pi\rho|v_R|^2 \equiv \Gamma. \quad (15)$$

Here ρ is the density of states of the reservoirs at the Fermi energy. We employ Γ as a unit of the energy in the following calculation.

We consider charge pumping from the reservoir L to the reservoir R against the chemical potential bias $\mu (> 0)$. The sign of the charge current is defined as positive when it flows from the reservoir L to the reservoir R (this corresponds to the direction that the electron is transferred from the reservoir R to the reservoir L). In the present setup, the pumping current is positive while the leakage current is negative (see Fig. 2).

B. Leakage current and Berry curvature

We introduce the dimensionless driving parameters as

$$X_1(t) = x(t) = \epsilon_d(t)/\Gamma, \quad (16)$$

$$X_2(t) = y(t) = \Gamma_L(t)/\Gamma. \quad (17)$$

For these definitions, the driving velocity $v = |d\mathbf{X}/dt|$ has a dimension of the energy, and should be taken as the *limited speed*, i.e., sufficiently smaller than the characteristic energy scale of the system, Γ . In the following calculation, we set it as $v = 0.1\Gamma$.

By the Meir-Wingreen formula²⁸, the normalized leakage current is calculated as

$$U(x, y) = \frac{e}{2\pi} \frac{2\Gamma y}{v} \int_{-\omega_0}^{\omega_0} d\omega \mathcal{A}(\omega), \quad (18)$$

where $\omega_0 = \mu\Gamma^{-1}/2$, e (< 0) is the elementary charge, and $\mathcal{A}(\omega)$ is a normalized spectral function

$$\mathcal{A}(\omega) = \frac{1}{(\omega - x)^2 + (1 + y)^2/4}. \quad (19)$$

Applying the adiabatic approximation in the Keldysh Green's function approach^{10,14,15}, the Berry curvature is calculated as

$$\begin{aligned} \Pi(x, y) = & -\frac{e}{2\pi} \left[y\mathcal{A}^2(\omega_0) + \frac{(1-y)}{2}\mathcal{A}^2(-\omega_0) \right. \\ & \left. - 2 \int_{-\omega_0}^{\omega_0} d\omega y(\omega - x)\mathcal{A}^3(\omega) \right]. \quad (20) \end{aligned}$$

C. Optimization by an ellipse contour

From the functional $Z[C, \mathcal{T}]$ given in Eq. (7), we can derive the differential equations to be satisfied for the optimized contour $C_{\text{opt}}(\mathcal{T})$ under the constraint of a fixed \mathcal{T} (see Appendix B). The optimized contour $C_{\text{opt}}(\mathcal{T})$ is then obtained by numerically solving these equations, and the

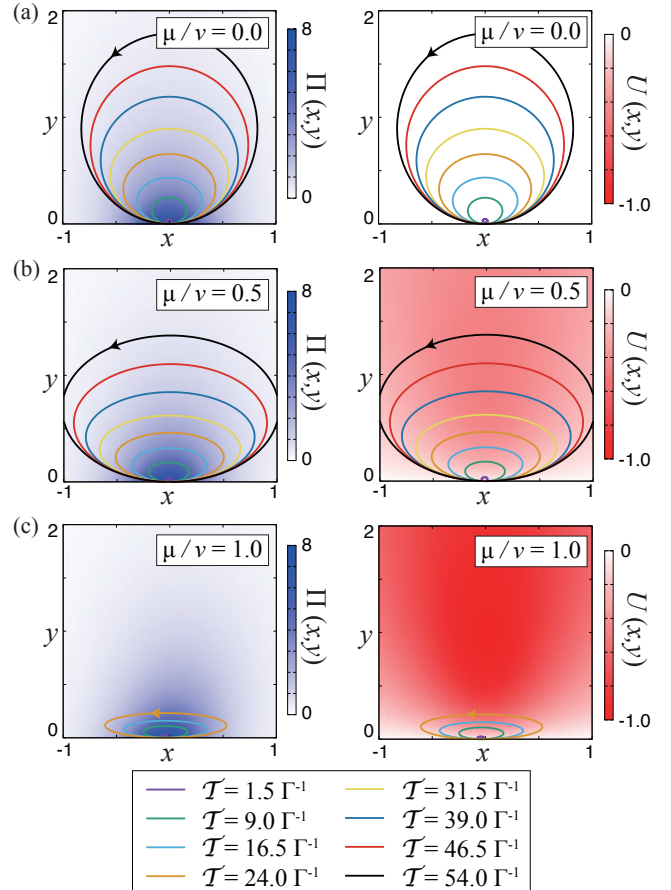


FIG. 3. Optimized ellipse contours for eight periods from $\mathcal{T} = 1.5\Gamma^{-1}$ to $\mathcal{T} = 54.0\Gamma^{-1}$. The velocity v is set to 0.1Γ and the chemical potential is set to (a) $\mu/v = 0.0$, (b) $\mu/v = 0.5$, and (c) $\mu/v = 1.0$. The left and right panels show the Berry curvature $\Pi(x, y)$ and the normalized leakage current $U(x, y)$ as a density plot. Both functions are represented in the unit of $|e|/2\pi$. For $\mu/v = 1.0$, charge pumping is possible for only four short-period contours, because the leakage current is always dominant for $\mathcal{T} > 28.5\Gamma^{-1}$.

pumping power $P(\mathcal{T}) = Z[C_{\text{opt}}, \mathcal{T}]/\mathcal{T}$ is obtained as a function of the period \mathcal{T} . For the present purpose, i.e., for showing the existence of the contour with the best pumping performance, it is sufficient to approximate the contour shape with some simple ones. In this section, we restrict the contour shape to an ellipse in the parameter space (x, y) , and optimize the parameters of the ellipse, i.e., a position of the center, lengths of the semi-major and semi-minor axes, and an angle of the semi-major axis, to maximize $Z[C, \mathcal{T}]$ (see Appendix C).

Fig. 3 shows the optimized elliptic contours for several pumping periods for three chemical potential biases: (a) $\mu/v = 0$, (b) $\mu/v = 0.5$, and (c) $\mu/v = 1.0$. The color density plots in the left and right panels show the Berry curvature $\Pi(x, y)$ and the normalized leakage current $U(x, y)$, respectively. The optimized contours (the solid lines) are the same in the left and right panels.

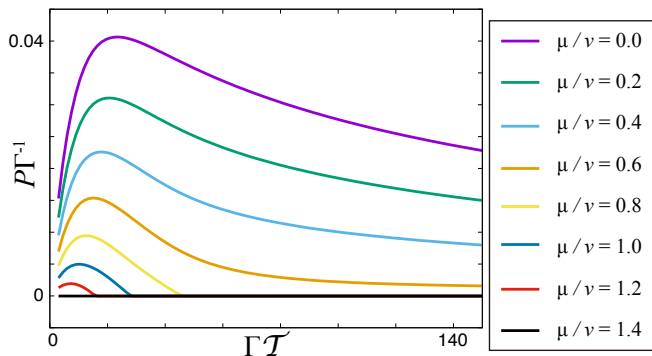


FIG. 4. The pumping power P for ellipse contours as a function of the period \mathcal{T} in the unit of $|e|/2\pi$. The chemical potential bias is set as eight values from $\mu/v = 0.0$ to 1.4. The velocity is set to $v = 0.1\Gamma$.

In the unbiased case (Fig. 3 (a)), the contour reflects only the profile of the Berry curvature in the parameter space since there is no leakage current. All the optimized contours touches the origin because the Berry curvature has its maximum at the origin. The contour gradually expands to the y -direction as the period increases. The Berry curvature is evaluated as $(1 + 4x^2)^{-2}\Pi(0,0)$ for $y = 0$, and to $(1 + y)^{-3}\Pi(0,0)$ for $x = 0$. Since $\Pi(x,y)$ decays faster in the x -direction, it is advantageous for charge pumping to extend the contour to the y -direction as the driving period \mathcal{T} increases.

In the biased cases (Fig. 3 (b) and (c)), the leakage current becomes finite. The leakage current is a monotonically increasing function of y for fixed x . Therefore, the optimized contour shrinks toward the line $y = 0$ to avoid loss of pumped charge due to the leakage as possible. The degree of the shrink becomes larger as the bias increases (Fig. 3 (b) and (c)). We should note that only four contours are presented in Fig. 3 (c). This indicates that charge pumping is impossible for long-period contours as the leakage dominates the charge pumping.

Figure 4 shows the pumping power $P(\mathcal{T}) = Z[C_{\text{opt}}, \mathcal{T}]/\mathcal{T}$ as a function of \mathcal{T} for several chemical potential biases. For the unbiased case ($\mu = 0$), the pumping power has a maximum at an optimal value of the period, \mathcal{T}_{opt} . The existence of the optimal period is explained as follows (see also Sec. I). The pumped charge ‘per cycle’ increases monotonically as the period \mathcal{T} becomes longer, because the area enclosed by the contour, on which the Berry curvature is integrated, is enlarged. Therefore, as the period becomes longer, the pumping power increases for $\mathcal{T} < \mathcal{T}_{\text{opt}}$. For longer-period pumping ($\mathcal{T} > \mathcal{T}_{\text{opt}}$), however, the pumping power is degraded since the denominator of the pumping power in Eq. (8) becomes effective. It should be noted that the optimal period \mathcal{T}_{opt} is of order of the inverse of the *limited speed* v (here, we set it as $v = 0.1\Gamma$). As the chemical potential bias μ increases, the pumping power is suppressed, and the optimal period \mathcal{T}_{opt} becomes shorter for $\mu/v < 1.2$. The charge pumping against the bias becomes impossible

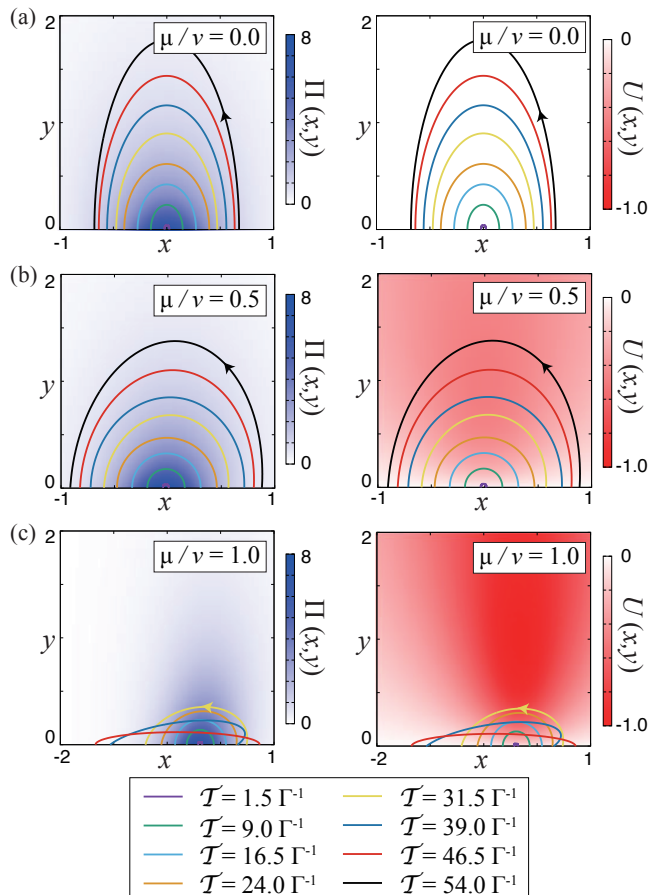


FIG. 5. Optimized half-ellipse contours for eight periods. The parameter setup is same with that in Fig. 3. The left panel and right panel show the Berry curvature and the normalized leakage current as a density plot in the unit of $|e|/2\pi$. For $\mu/v = 1.0$, charge pumping is possible only for seven short-period contours, because the leakage current is always dominant for $\mathcal{T} > 54.0\Gamma^{-1}$.

in the whole region for $\mu/v = 1.4$.

D. Optimization by a half-ellipse contour

The existence of the optimal period for charge pumping is the main result of this paper. This result should not depend on the choice of the contour shape. To show this, we consider the half-ellipse contour (for details, see Appendix C), and compare the results with those for the ellipse contour.

Figure 5 (a)-(c) present the optimized contours for several pumping periods. The density plots of the Berry curvature and the leakage current are shown in the left and right panels. The parameters are the same with that of the ellipse one. The overall features are common as the results for the elliptic contours. For the unbiased case (Fig. 5 (a)), the contour enclose the region near the origin, at which the Berry curvature has a maximum value.

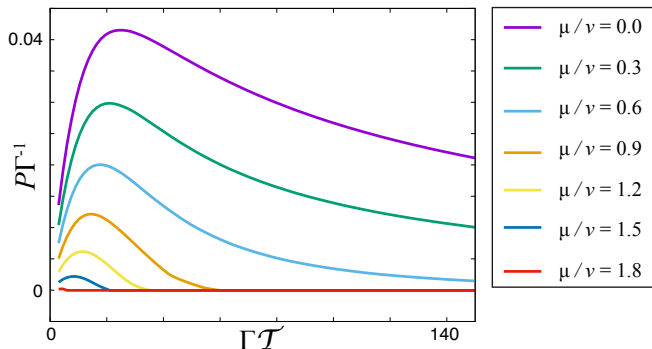


FIG. 6. The pumping power P for half-ellipse contours as a function of the period \mathcal{T} in the unit of $|e|/2\pi$. The chemical potential bias is set as seven values from $\mu/v = 0.0$ to 1.8. The velocity is set to $v = 0.1\Gamma$.

As the chemical potential bias μ increases (Fig. 5 (b) and (c)), the contour shrinks toward the line $y = 0$ to avoid the region where the leakage current is large. The center and the angle of the half-elliptic contours are changed more clearly than the elliptic contours, reflecting small change of the Berry curvature and the leakage current.

Figure 6 shows the pumping power of the half-ellipse contours for several biases. While the qualitative feature is the same as the elliptic case, the pumping power against the bias is improved, and become possible up to $\mu/v \sim 1.8$, which is larger than the ellipse case. The maximum value of the pumping power, $P_{\text{opt}} \simeq 0.041$, is slightly larger than $P_{\text{opt}} \simeq 0.040$ for the ellipse case.

IV. SUMMARY

In this paper, we have studied the optimization of the performance of adiabatic pumping. We have formulated the optimized contour under a fixed pumping period assuming that the velocity of the parameter driving is constant. We have actually discussed the optimal contour in charge pumping via a single-level quantum dot by approximating the shapes of the contours into elliptic and half-elliptic ones. We have shown that the pumping power indeed takes a maximum at a certain optimal period of driving in the unbiased case. We have also shown that the pumping against the chemical potential bias is possible for a small bias even though there exists the leakage current in the direction opposite to the charge pumping. Since the optimal contour and period are determined by a simple mechanism, we expect that these features for a specific example are common for general transport systems.

We have considered a simple system for which the adiabatic condition on the driving velocity is obtained easily. It is a future problem to derive the detailed condition for the adiabatic pumping, and to improve the formulation for optimization of pumping.

ACKNOWLEDGMENTS

The authors acknowledge T. Tamaya for useful comments on the manuscript. M.H. acknowledges financial support provided by the Advanced Leading Graduate Course for Photon Science. T.K. was supported by JSPS Grants-in-Aid for Scientific Research (No. JP24540316 and JP26220711).

Appendix A: Adiabatic approximation

In this appendix, we briefly derive Eqs. (1)-(3) for general systems including interacting electron systems (see Refs. 10, 14, and 15 for detailed derivation). For simplicity, we assume that the time-dependent parameter vector $\mathbf{X}(t)$ is driven in the sinusoidal manner:

$$X_n(t) = X_{n,0} + \delta X_n \sin(\omega t + \phi_n). \quad (\text{A1})$$

Here $X_{n,0}$, δX_n and ϕ_n are a center, an amplitude and a phase of the sinusoidal parameter driving, and ω is a pumping frequency. Although this assumption seems to oversimplify the problem, it captures the essence of the adiabatic approximation. When the parameter vector $\mathbf{X}(t)$ is driven slowly, we can consider adiabatic expansion for the time-dependent current $J(t)$ as

$$J(t) = J^{(0)} + \sum_n J_n^{(1)} \dot{X}_n(t) + \sum_n J_n^{(2,1)} \ddot{X}_n(t) + \sum_{n,m} J_{nm}^{(2,2)} \dot{X}_n(t) \dot{X}_m(t) + \dots \quad (\text{A2})$$

In the adiabatic approximation, the leading and the next leading term, $J^{(0)}$ and $J_n^{(1)}$, are taken into account and the rest terms are neglected. To justify this approximation, the pumping frequency and the pumping amplitude must satisfy the following condition:

$$J_n^{(2,1)} \omega^2 \delta X_n, J_n^{(2,2)} \omega^2 \delta X_n \delta X_m \ll J_{n'}^{(1)} \omega \delta X_{n'}, \quad (\text{A3})$$

for arbitrary m , n and n' . This condition implies the trade-off between the amplitude and the frequency of pumping; the pumping frequency should be smaller if the amplitude of driving becomes larger, and vice versa. This relation indicates that the product of them, $\omega \delta \mathbf{X} \simeq \dot{\mathbf{X}}$, has an upper bound, which we call the *limited speed*. For the dimensionless parameter vector \mathbf{X} , this *limited speed* is taken as much smaller than the characteristic energy scale of the system.

Let us see the detail of the leading and next leading terms. The leading contribution corresponds to the steady-state contribution,

$$J^{(0)}(t) = j[\mathbf{X}(t)] = J(t)|_{\text{st.}} \quad (\text{A4})$$

Here $O|_{\text{st.}}$ denotes the steady-state average of the observable O under a fixed parameter vector $\mathbf{X}(t)$. The next

leading contribution corresponds to contribution of the adiabatic pumping,

$$J_n^{(1)} = \pi_n[\mathbf{X}(t)] = \left. \frac{\partial J(t)}{\partial \dot{X}_n(t)} \right|_{\text{st.}}, \quad (\text{A5})$$

where $\pi_n[\mathbf{X}(t)]$ is called the Berry connection. The amount of charge or heat transferred in one cycle is described as a sum of the steady and adiabatic part:

$$Q = Q^{\text{st.}} + Q^{\text{ad.}}, \quad (\text{A6})$$

$$Q^{\text{st.}} = \int_0^{\mathcal{T}} dt J^{(0)}(t), \quad (\text{A7})$$

$$Q^{\text{ad.}} = \int_0^{\mathcal{T}} dt J^{(1)}(t) = \oint_C d\mathbf{X} \cdot \boldsymbol{\pi}, \quad (\text{A8})$$

where \mathcal{T} is a period of pumping, which equals to $2\pi\omega^{-1}$ in this case, and C is a closed contour in the parameter space. For the two-parameter driving $\mathbf{X} = (X_1, X_2)$, we can rewrite the formula for $Q^{\text{ad.}}$ using the Stokes theorem as

$$Q^{\text{ad.}} = \int_A dX_1 dX_2 \Pi(\mathbf{X}), \quad (\text{A9})$$

where $\Pi(\mathbf{X}) = \partial_{X_1}\pi_2(\mathbf{X}) - \partial_{X_2}\pi_1(\mathbf{X})$ is the Berry curvature, and A is the area enclosed by the contour C . Thus, we obtain Eqs. (1)-(3).

As an example, let us consider charge pumping via a non-interacting electron system (the Brouwer's formula⁷). The amount of pumped charge from the reservoir L to the reservoir R is then written in terms of the scattering matrix as

$$\pi_m[\mathbf{X}(t)] = \frac{e}{\pi} \sum_{r=L,R} \text{Im} \left[\frac{\partial S_{Lr}}{\partial X_m} S_{Lr}^\dagger \right]. \quad (\text{A10})$$

Here $S_{r_1 r_2}$ denotes a scattering matrix element from the reservoir r_1 to r_2 . Although the scattering theory is not applicable to interacting electron systems, Keldysh Green's function method can generalize this formula even for interacting systems, and gives the same form as Eqs. (1)-(3) (for details, see Refs. 10 and 15). It is also worth noting that one can obtain the same geometrical formalism in the incoherent transport system by using Master equation approach¹⁷.

Appendix B: Stationary equation

In this appendix, we derive the stationary equation to optimize $Z[C, \mathcal{T}]$. Let us consider small variation of the contour, $C \rightarrow C + \delta C$ (see Fig. 7). This is described by variation of the parameter vector, $\mathbf{X}(s) \rightarrow \mathbf{X}(s) + \delta\mathbf{X}(s)$. Here we describe the variation $\delta\mathbf{X}(s)$ by a linear combination of a tangent vector $\mathbf{t}(s)$ and a normal vector $\mathbf{n}(s)$ of contour C as

$$\delta\mathbf{X}(s) = \delta t(s)\mathbf{t}(s) + \delta n(s)\mathbf{n}(s). \quad (\text{B1})$$

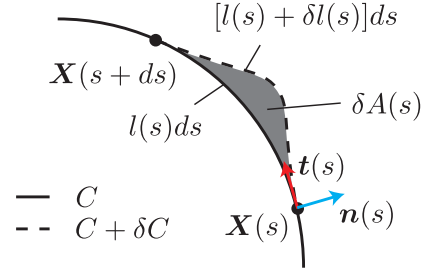


FIG. 7. A schematic of contour variation. By adding a variation $\delta\mathbf{X}(s)$ within the infinitesimal section $[s, s + ds]$, the contour C (solid line) changes into the contour $C + \delta C$ (dotted line). By this variation, the length of the contour increases from $l(s)ds$ to $[l(s) + \delta l(s)]ds$. The area of the contour also increases by $\delta A(s)$. The red and blue arrows denote the tangent vector $\mathbf{t}(s)$ and the normal vector $\mathbf{n}(s)$ of the contour C , respectively.

We choose the orientation of $\mathbf{n}(s)$ so that the area A enclosed by C increase when $\delta n(s)$ is positive. The difference of $Z[C, \mathcal{T}]$ induced by this variation is evaluated by three contributions as follows:

$$\begin{aligned} \delta Z[C, \mathcal{T}] &= Z[C + \delta C, \mathcal{T}] - Z[C, \mathcal{T}] \\ &\simeq \int_0^1 ds \left\{ (U[\mathbf{X}(s)] + \lambda v^{-1})\delta l(s) \right. \\ &\quad \left. + l(s)\delta U[\mathbf{X}(s)] + \Pi(\mathbf{X})\delta A(s) \right\}. \end{aligned} \quad (\text{B2})$$

Here $\delta A \simeq \delta n(s)l(s)$ is the variation of the area, and $\delta l(s)$ is a difference of the line element,

$$\begin{aligned} \delta l(s) &= \left| \frac{d(\mathbf{X}(s) + \delta\mathbf{X}(s))}{ds} \right| - \left| \frac{d\mathbf{X}(s)}{ds} \right| \\ &\simeq \dot{\delta t}(s) + (\mathbf{t}(s) \cdot \dot{\mathbf{n}}(s))\delta n(s). \end{aligned} \quad (\text{B3})$$

Hereafter we use the notation, $\dot{f} = df/ds$. The variation of the normalized leakage current is written as

$$\begin{aligned} \delta U[\mathbf{X}(s)] &= U[\mathbf{X}(s) + \delta\mathbf{X}(s)] - U[\mathbf{X}(s)] \\ &\simeq \partial_t U[\mathbf{X}(s)]\delta t(s) + \partial_n U[\mathbf{X}(s)]\delta n(s). \end{aligned} \quad (\text{B4})$$

Here $\partial_{t/n}$ is a directional derivative along the tangent/normal direction, respectively. The stationary condition, $\delta Z[C, \mathcal{T}] = 0$, leads to the equation

$$\begin{aligned} (\mathbf{t}(s) \cdot \dot{\mathbf{n}}(s))(U[\mathbf{X}(s)] + \lambda v^{-1}) \\ + l(s)\partial_n U[\mathbf{X}(s)] + l(s)\Pi[\mathbf{X}(s)] = 0. \end{aligned} \quad (\text{B5})$$

By solving this equation, we can obtain the contour C , which maximizes the amount of pumping under a fixed period, $Z[C, \mathcal{T}]$.

Appendix C: Representation of ellipse and half-ellipse

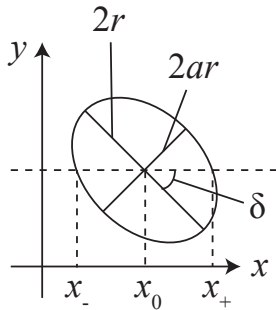


FIG. 8. Parametrization of an elliptic contour.

We describe the ellipse contour by the parametric representation as following (see Fig. 8):

$$x(s) = r(s) \cos 2\pi s + x_0, \quad (\text{C1})$$

$$y(s) = r(s) \sin 2\pi s + y_0, \quad (\text{C2})$$

where

$$r(s) = \frac{r}{\sqrt{\cos^2(2\pi s + \delta) + a^2 \sin^2(2\pi s + \delta)}}. \quad (\text{C3})$$

The parameters, x_0 , y_0 , and δ , vary in the condition that all the points on the contour are located in the upper plane ($y \geq 0$).

We describe the half-ellipse by setting y_0 to zero, and by restricting the parameter s in the range of $0 \leq s \leq 0.5$:

$$x(s) = r(s) \cos 2\pi s + x_0, \quad (\text{C4})$$

$$y(s) = r(s) \sin 2\pi s. \quad (\text{C5})$$

The remaining contour is a straight line described by

$$x(s) = (x_+ - x_-)(s - 0.5) + x_-, \quad (\text{C6})$$

$$y(s) = 0. \quad (\text{C7})$$

for $0.5 \leq s \leq 1$, where x_+ and x_- are the cross points between the ellipse and the horizontal line through the center (see Fig. 8).

-
- ¹ D. J. Thouless, *Phys. Rev. B* **27**, 6083 (1983).
 - ² L. P. Kouwenhoven, A. T. Johnson, N. C. van der Vaart, C. J. P. M. Harmans, and C. T. Foxon, *Phys. Rev. Lett.* **67**, 1626 (1991).
 - ³ H. Pothier, P. Lafarge, C. Urbina, D. Esteve, and M. H. Devoret, *EPL* **17**, 249 (1992).
 - ⁴ M. Büttiker, A. Prêtre, and H. Thomas, *Phys. Rev. Lett.* **70**, 4114 (1993).
 - ⁵ M. Büttiker, H. Thomas, and A. Prêtre, *Zeitschrift für Physik B Condensed Matter* **94**, 133 (1994).
 - ⁶ A. Prêtre, H. Thomas, and M. Büttiker, *Phys. Rev. B* **54**, 8130 (1996).
 - ⁷ P. W. Brouwer, *Phys. Rev. B* **58**, R10135 (1998).
 - ⁸ I. L. Aleiner and A. V. Andreev, *Phys. Rev. Lett.* **81**, 1286 (1998).
 - ⁹ O. Entin-Wohlman, A. Aharony, and Y. Levinson, *Phys. Rev. B* **65**, 195411 (2002).
 - ¹⁰ J. Splettstoesser, M. Governale, J. König, and R. Fazio, *Phys. Rev. Lett.* **95**, 246803 (2005).
 - ¹¹ J. Splettstoesser, M. Governale, J. König, and R. Fazio, *Phys. Rev. B* **74**, 085305 (2006).
 - ¹² S. Andergassen, V. Meden, H. Schoeller, J. Splettstoesser, and M. R. Wegewijs, *Nanotechnology* **21**, 272001 (2010).
 - ¹³ J. P. Pekola, O.-P. Saira, V. F. Maisi, A. Kemppinen, M. Möttönen, Y. A. Pashkin, and D. V. Averin, *Rev. Mod. Phys.* **85**, 1421 (2013).
 - ¹⁴ M. Hasegawa and T. Kato, *J. Phys. Soc. Jpn.* **86**, 024710 (2017).
 - ¹⁵ M. Hasegawa and T. Kato, *J. Phys. Soc. Jpn.* **87**, 044709 (2018).
 - ¹⁶ J. Ren, P. Hänggi, and B. Li, *Phys. Rev. Lett.* **104**, 170601 (2010).
 - ¹⁷ S. Juergens, F. Haupt, M. Moskalets, and J. Splettstoesser, *Phys. Rev. B* **87**, 245423 (2013).
 - ¹⁸ F. Haupt, M. Leijnse, H. L. Calvo, L. Classen, J. Splettstoesser, and M. R. Wegewijs, *Phys. Status Solidi B* **250**, 2315 (2013).
 - ¹⁹ B. Karimi and J. P. Pekola, *Phys. Rev. B* **94**, 184503 (2016).
 - ²⁰ G. Benenti, G. Casati, K. Saito, and R. Whitney, *Phys. Rep.* **694**, 1 (2017).
 - ²¹ T. Yuge, T. Sagawa, A. Sugita, and H. Hayakawa, *J. Stat. Phys.* **153**, 412 (2013).
 - ²² S. Nakajima and Y. Tokura, *J. Stat. Phys.* **169**, 902 (2017).
 - ²³ M. Esposito, M. A. Ochoa, and M. Galperin, *Phys. Rev. Lett.* **114**, 080602 (2015).
 - ²⁴ M. A. Ochoa, N. Zimbovskaya, and A. Nitzan, *Phys. Rev. B* **97**, 085434 (2018).
 - ²⁵ C. Chamon, E. R. Mucciolo, L. Arrachea, and R. B. Capaz, *Phys. Rev. Lett.* **106**, 135504 (2011).
 - ²⁶ R. S. Whitney, *Phys. Rev. Lett.* **112**, 130601 (2014).
 - ²⁷ N. Shiraishi, K. Saito, and H. Tasaki, *Phys. Rev. Lett.* **117**, 190601 (2016).
 - ²⁸ Y. Meir and N. S. Wingreen, *Phys. Rev. Lett.* **68**, 2512 (1992).